

Transmembrane Segments Prevent Surface Expression of Sodium Channel Na_v1.8 and Promote Calnexin-dependent Channel Degradation^{*[5]}

Received for publication, May 10, 2010, and in revised form, July 20, 2010. Published, JBC Papers in Press, August 18, 2010, DOI 10.1074/jbc.M110.143024

Qian Li, Yuan-Yuan Su, Hao Wang, Lei Li, Qiong Wang, and Lan Bao¹

From the Laboratory of Molecular Cell Biology, Institute of Biochemistry and Cell Biology, Shanghai Institutes for Biological Sciences, Chinese Academy of Sciences, Shanghai 200031, China

The voltage-gated sodium channel (Na_v)_{1.8} contributes substantially to the rising phase of action potential in small dorsal root ganglion neurons. Na_v1.8 is majorly localized intracellularly and its expression on the plasma membrane is regulated by exit from the endoplasmic reticulum (ER). Previous work has identified an ER-retention/retrieval motif in the first intracellular loop of Na_v1.8, which prevents its surface expression. Here we report that the transmembrane segments of Na_v1.8 also cause this channel retained in the ER. Using transferrin receptor and CD8 α as model molecules, immunocytochemistry showed that the first, second, and third transmembrane segments in each domain of Na_v1.8 reduced their surface expression. Alanine-scanning analysis revealed acidic amino acids as critical factors in the odd transmembrane segments. Furthermore, co-immunoprecipitation experiments showed that calnexin interacted with acidic amino acid-containing sequences through its transmembrane segment. Overexpression of calnexin resulted in increased degradation of those proteins through the ER-associated degradation pathway, whereas down-regulation of calnexin reversed the phenotype. Thus our results reveal a critical role and mechanism of transmembrane segments in surface expression and degradation of Na_v1.8.

Voltage-gated sodium channels (Na_v)² play a fundamental role in the excitable cells. They are required to generate and propagate the action potential. Although the intact channels are composed of α and β subunits, the highly glycosylated α subunit alone is capable of forming the functional sodium-selective channel. So far 10 α subunit genes have been cloned in mammals, designated Na_v1.1–Na_v1.9 and an atypical Na_x. These different channels have homologous sequences and show subtle differences in channel properties (1–4). Voltage-gated sodium channel α subunit consists of four homologous

domains (I–IV) linked by three intracellular loops and each domain contains six transmembrane segments (S1–S6). Na_v1.8 is a tetrodotoxin-resistant sodium channel preferentially expressed in nociceptive dorsal root ganglion (DRG) neurons (5). Studies from knock-out mice and antisense oligodeoxynucleotide suggest an important role of Na_v1.8 in development of inflammatory and neuropathic pain (6–9).

Ion channel folding and assembly is typically a tightly controlled process to ensure properly folded and fully assembled complex expressing on the cell surface. Endoplasmic reticulum (ER) quality control is one key mechanism involved in this process, which results in ER localization of the aberrantly folded proteins or incompletely assembled complexes. These proteins contain potential ER-retention/retrieval signals in the cytoplasmic domains (10–14) and/or in the transmembrane segments (15–20) and/or in the extracellular domains (21, 22), which confer their ER localization until the signals are sterically masked by its partners or undergo conformational changes to become nonfunctional. To avoid the potentially catastrophic consequence of misfolded protein accumulation, ER-retained products are commonly destroyed by ER-associated degradation (ERAD) destined for the cytoplasmic ubiquitin-proteasome pathway. So far, at least three different mechanisms are defined to detect the structural features of these substrates, including calnexin/calreticulin cycle, BiP recognition, and the protein-disulfide isomerases pathway (23–26). The intensively studied ER chaperon calnexin is a type I membrane protein. Calnexin selectively interacts with glycoproteins containing an *N*-linked oligosaccharide intermediate, Glc₁Man₃GlcNAc₂, which possesses a single terminal glucose residue to assist correct folding (27, 28). Terminally misfolded glycoproteins will be targeted for ERAD by releasing from calnexin interaction (29).

Na_v1.8 exerts its function of supporting action potential conduction in the C-type small DRG neurons on the plasma membrane (30). Interestingly, several groups have reported that Na_v1.8 is mainly localized intracellularly in both DRG neurons and transfected heterologous cells (31–33). In addition, we have previously reported that Na_v1.8 is mainly localized in the ER and contains an ER-retention/retrieval signal (⁴⁹⁵RRR⁴⁹⁷) in the first intracellular loop that regulates trafficking of Na_v1.8 to the plasma membrane (31). However, the surface expression of Na_v1.8 was increased only 3-fold when the RRR motif was mutated into alanine, indicating the involvement of the remaining part of Na_v1.8 in its ER localization.

* This work was supported by National Basic Research Program of China Grants 2007CB914501 and 2010CB912001, National Natural Science Foundation of China Grants 30570574 and 30623003.

[5] The on-line version of this article (available at <http://www.jbc.org>) contains supplemental Table S1.

¹ To whom correspondence should be addressed: 320 Yue-Yang Rd., Shanghai 200031, China. Tel.: 86-21-54921369; Fax: 86-21-54921369; E-mail: baolan@sibs.ac.cn.

² The abbreviations used are: Na_v, voltage-gated sodium channels; CHX, cycloheximide; DRG, dorsal root ganglion; ER, endoplasmic reticulum; ERAD, ER-associated degradation; Na_v1.8, voltage-gated sodium channel 1.8; TFR1, transferrin receptor 1; CFTR, cystic fibrosis transmembrane conductance regulator; AchR, acetylcholine receptor.

Trafficking Regulation for Na_v1.8

In this study, we focused on the role of transmembrane segments of Na_v1.8 in its ER localization. We found that both the odd and even transmembrane segments contributed to channel localization in ER, and the acidic amino acid in the odd transmembrane segments produced the ER localization effect. Moreover, calnexin recognized this sequence through its transmembrane segment and accelerated the degradation of chimeric protein and Na_v1.8. Thus, our findings define a novel mechanism for ER localization of Na_v1.8 and decipher a previously unrecognized role for calnexin in the degradation of transmembrane proteins.

EXPERIMENTAL PROCEDURES

Plasmid Construction and siRNA—The plasmids containing full-length rat Na_v1.8, Myc-CD8 α , and Myc-CD8 α -KKTN have been described by our previous study (31). Na_v1.8^{IIS1-D663A/P664A/E667A}-GFP, Na_v1.8^{IIS3-N729A/I730A/D732A}-GFP, Na_v1.8^{IIS3-D1223A}-GFP, Na_v1.8^{IVS1-D1480A}-GFP, and Na_v1.8^{IVS3-D1544A}-GFP plasmids were generated by PCR from Na_v1.8-GFP using the KOD-Plus mutagenesis kit (Toyobo, Shiga, Japan). The primers used were listed in supplemental Table S1.

TFR1 plasmid was a gift from Dr. Xiang-jun Tong (Peking University). Then a FLAG tag was added into the N terminus of TFR1 with the following primers: 5'-catgctcgagatggactacag-gacgacgatgacaaggaattcagaatgatggatcaag-3' and 5'-ctaggatc-caaactcattgtcaatgtcccaaac-3'. The amplified DNA fragment was inserted into pMyc (a modified vector of pEGFP-N3 in which the GFP tag was replaced by the Myc tag). So TFR1 plasmid contained a FLAG tag in the N terminus and a Myc tag in the C terminus. The classical internalization signal YTRF (34) was deleted to get the plasmid FLAG-TFR1-Myc using KOD-Plus mutagenesis kit with following primers: 5'-tacttgccgagc-caggcttgacaatggttctccacc-3' and 5'-ggtggagaaccattgtcaagcctg-gctcggaagta-3'. Then various plasmids encoding chimeric proteins were generated by substituting the transmembrane segment of TFR1 with the transmembrane segments of Na_v1.8 by PCR using the primers listed in supplemental Table S1. Myc-CD8 α -derived plasmids were obtained by replacing the transmembrane segment of CD8 α with transmembrane segments of Na_v1.8 or calnexin using the primers listed in supplemental Table S1.

Calnexin was amplified from the HEK293 cDNA library and cloned into the pHA vector (a modified vector of pEGFP-N3 vector in which the GFP tag is replaced by the HA tag). Plasmids of calnexin(Δ C)-HA and calnexin mutant, which were resistant to siRNA, were generated directly by PCR. The primers used were listed in supplemental Table S1. siRNA specific for human calnexin and the scrambled siRNA were synthesized according to sequences in the previous study (35).

Calnexin shRNA and scramble shRNA plasmids were generated by direct synthesis and insertion of the corresponding sequences into pSUPER vector. The primers used were listed in supplemental Table S1.

Cell Culture and Transfection—African green monkey kidney COS-7 cells were obtained from the American Type Culture Collection (ATCC; Manassas, VA) and grown in DMEM (Invitrogen) supplemented with 10% fetal bovine serum (Invitrogen). COS-7 cells were transfected with various plas-

mids using Lipofectamine 2000 (Invitrogen) according to the manufacturer's instruction. Two days after transfection, the cells were used for immunocytochemistry. HEK293 cells derived from ATCC were grown in minimal essential medium (Invitrogen) supplemented with 10% fetal bovine serum. HEK293 cells were transiently transfected with plasmids using the calcium phosphate method and analyzed for different assays after 2 days. HEK293 cells were transiently transfected with siRNAs using Lipofectamine 2000 and analyzed for immunoblotting after 2 days. HEK293 cells stably expressing FLAG-TFR1(TM_{IVS3})-Myc, FLAG-TFR1(TM_{IVS3-D1544A})-Myc, or Na_v1.8-GFP or Na_v1.8^{IVS3-D1544A}-GFP were selected by growth in the presence of 1000 μ g/ml of G418 (Amresco, Solon, OH). Colonies expressing FLAG-TFR1(TM_{IVS3})-Myc or FLAG-TFR1(TM_{IVS3-D1544A})-Myc were directly picked up and Na_v1.8-GFP or Na_v1.8^{IVS3-D1544A}-GFP-containing colonies were picked up by FACS Calibur instrument (BD Biosciences). Stable cell lines were then chosen based on persistent expression and correct subcellular localization judged by Western blotting and immunocytochemistry. Stable cell lines were grown in the presence of 500 μ g/ml of G418 for maintenance.

Preparation of Dissociated DRG Neurons—Neurons were dissociated from DRG of adult male Sprague-Dawley rats (body weight 120–150 g; Shanghai Center of Experimental Animals, Chinese Academy of Sciences) according to the policy of the Society for Neuroscience on the use of animals. The experiment was approved by the Committee of Use of Laboratory Animals and Common facility, Institute of Biochemistry and Cell Biology, Chinese Academy of Sciences. Briefly, the rats were deeply anesthetized and sacrificed. Freshly dissected DRGs were digested in DMEM containing 1 mg/ml of collagenase type 1A, 0.4 mg/ml of trypsin type I, and 0.1 mg/ml of DNase I (all from Sigma) at 37 °C for 35 min. Then, DRGs were triturated with glass pipettes and cultured in DMEM supplemented with 10% fetal bovine serum for drug treatment.

Drug Treatment—HEK293 cells and dissociated DRG neurons were incubated with 100 μ g/ml of cycloheximide (CHX) (Sigma) in culture medium for 0.5, 1, 2, and 12 h and then harvested for Western blotting. Treatment of cells with 10 μ M MG132 (Sigma) and 100 μ M leupeptin (Roche Applied Science) were performed for 6 h. The control cells were treated with DMSO, the vehicle used for drug preparation.

Cell-surface Biotinylation and Western Blotting—Cell-surface biotinylation experiment was modified according to our previous protocol (36). Briefly, transiently transfected HEK293 cells were incubated with Sulfo-NHS-biotin (Pierce) in cold PBS for 30 min at 4 °C and 10 mM glycine was added afterward to stop the reaction. Then cells were harvested in RIPA lysis buffer (150 mM NaCl, 30 mM HEPES, 10 mM NaF, 1% Triton, 0.01% SDS, 0.1 mM PMSF, 1 mg/ml of pepstatin A, and 1 mg/ml of leupeptin) and lysed for 1 h at 4 °C. Biotin-labeled proteins were precipitated overnight with Immopure Immobilized Neutravidin (Pierce). Beads were then washed three times with RIPA buffer and incubated at 50 °C for 20 min in SDS-PAGE loading buffer.

The samples used for Western blotting were separated on SDS-PAGE, transferred, probed with specific antibodies, and visualized with enhanced chemiluminescence (Amersham Bio-

sciences, UK). The primary antibodies were used, including mouse antibodies against GFP (1:1,000; Roche, Indianapolis, IN), Myc (1:5000; home-made) and actin (1:10,000; Chemicon, Single Oak Drive Temecula, CA), and rabbit antibodies against HA (1:2,000; Sigma), calnexin (1:10,000; Sigma), and Na_v1.8 (1:2,000; Alomone Labs Ltd, Jerusalem, Israel). The immunoreactive bands were quantified by Image-Pro Plus software (Media Cybernetics Inc., Bethesda, MD). Statistical results were analyzed using Sigma Plot 10.0 (Systat Software Inc., Chicago, IL) based on at least three independent experiments. All data were shown as mean ± S.E. and analyzed by Student's *t* test.

Co-immunoprecipitation—HEK293 cells were lysed in recovery buffer (1% Triton X-100, 50 mM Tris-HCl, pH 7.5, and 150 mM NaCl) and the lysate samples were incubated overnight at 4 °C with each antibody as described in the figure legends, followed by incubation with protein G-Sepharose beads (Amersham Biosciences) for 2 h at 4 °C. The immunoprecipitates were washed efficiently with recovery buffer and analyzed by Western blotting. The experiment was repeated at least three times.

Immunocytochemistry—The transfected COS-7 cells grown in the glass coverslips were fixed with 4% paraformaldehyde at 4 °C for 15 min. For co-localization staining of FLAG-TFR1(TM_{IVS3})-Myc with the ER marker calnexin, COS-7 cells were incubated overnight with mouse antibody against Myc (1:500) and rabbit antibody against calnexin (1:1000) at 4 °C. The cells were incubated with a mixture of donkey antibody against mouse conjugated with FITC (1:100; Jackson ImmunoResearch, West Grove, PA) and donkey antibody against rabbit conjugated with Cy3 (1:100; Jackson ImmunoResearch).

For non-permeabilized staining of surface proteins, live COS-7 cells transfected with FLAG-TFR1-Myc chimeric proteins or Myc-CD8α chimeric proteins were first labeled with mouse antibody against Myc (1:100) diluted in Ca²⁺/Mg²⁺ PBS for 1 h at 4 °C. Then, the donkey antibody against mouse conjugated with FITC was incubated for 30 min at 4 °C. For permeabilized staining of total proteins, the cells were fixed and incubated with rabbit antibody against Myc (1:500 in 0.3% Triton X-100; Sigma) overnight at 4 °C. The donkey antibody against rabbit conjugated with Cy3 was incubated for 45 min at 37 °C. Finally, the cells were examined using a ×63 oil lens (numerical aperture 1.32) with a Leica DMRE microscope and images were captured with the SP2 laser scanning confocal system at ~20 °C (Leica, Germany). The immunofluorescence intensities of surface and total proteins were quantified by Image-Pro Plus software and the statistical results were analyzed using Sigma Plot 10.0 based on at least 45 cells from three independent experiments. All data were shown as mean ± S.E. and analyzed by paired Student's *t* test.

RESULTS

The Transmembrane Segments of Na_v1.8 Prevent Surface Expression of Chimeric Protein—Na_v1.8 consists of four homologous domains termed I–IV. Within each domain, there are six transmembrane segments called S1–S6 (Fig. 1A). To determine whether the transmembrane segments of Na_v1.8 contribute to ER localization of this channel, we detected their ER-localization activity, respectively. Considering the different orientation

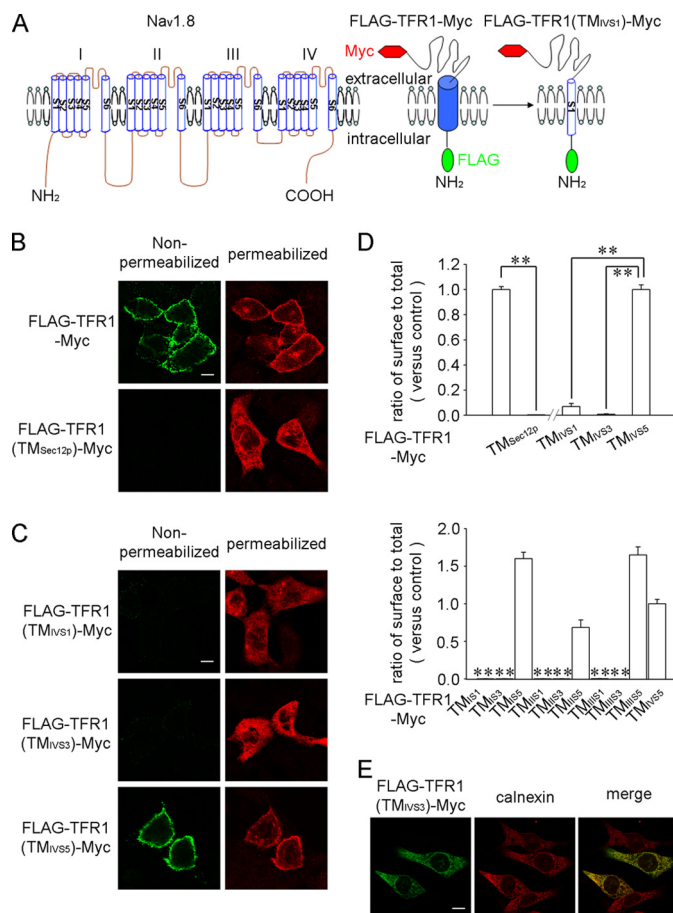


FIGURE 1. The odd transmembrane segments of Na_v1.8 retain chimeric proteins in the ER. A, schematic diagrams showing the structure of Na_v1.8, TFR1, and TFR1 chimeric proteins with the transmembrane segment substituted with the odd transmembrane segment of Na_v1.8. B and C, the TFR1 screening system was verified and the effects of odd transmembrane segments in the fourth domain of Na_v1.8 on the surface expression of chimeric proteins were analyzed. The COS-7 cells were transfected with plasmids expressing FLAG-TFR1-Myc or FLAG-TFR1(TM_{Sec12p})-Myc or FLAG-TFR1(TM_{IVS1})-Myc, FLAG-TFR1(TM_{IVS3})-Myc, or FLAG-TFR1(TM_{IVS5})-Myc. The non-permeabilized (green) and permeabilized (red) immunofluorescence staining was carried out with mouse- and rabbit-derived antibodies against Myc, respectively. The representative images were obtained from at least three independent experiments. Scale bar, 10 μm. D, the ratio (mean ± S.E.) of immunofluorescence intensity of surface (non-permeabilized) versus total (permeabilized) protein was calculated and then the data plotted as a percentage of control based on at least 45 cells in three experiments. **, *p* < 0.01 versus control cells or cells transfected with the plasmid of FLAG-TFR1(TM_{IVS3})-Myc. E, the expressed FLAG-TFR1(TM_{IVS3})-Myc is co-localized with the ER marker calnexin. The plasmid expressing FLAG-TFR1(TM_{IVS3})-Myc was transfected into COS-7 cells. The transfected cells were stained with antibody against Myc (green) and calnexin (red). Scale bar, 10 μm.

in the membrane for odd and even transmembrane segments, we constructed two systems of chimeric protein: type I membrane protein CD8α for the even transmembrane segments and type II membrane protein transferrin receptor 1 (TFR1) for the odd transmembrane segments. The transmembrane segments of CD8α or TFR1 were substituted with the odd or even transmembrane segments of Na_v1.8, respectively (Figs. 1A and 2A). The Myc tag was added to the C terminus of TFR1 or the N terminus of CD8α, being exposed extracellularly for non-permeabilized surface labeling of chimeric proteins. After expressing these chimeric proteins in COS-7 cells, we visualized their subcellular localization and surface expression using immunostaining.

Trafficking Regulation for Na_v1.8

First we checked ER-localization activity of the transmembrane segments in the fourth domain of Na_v1.8. In COS-7 cells, the expressed FLAG-TFR1-Myc with the internalization sequence YXRF deleted (34) displayed distinct expression on the cell surface (Fig. 1B). The yeast Sec12p is a type II membrane protein localized in the ER (37). When the transmembrane segment of TFR1 was substituted with that of Sec12p, the resulting chimeric protein FLAG-TFR1(TM_{Sec12p})-Myc exhibited a typical reticulum-like localization and greatly reduced surface expression (Fig. 1B), suggesting a well established screening system. We then replaced the transmembrane segment of TFR1 with the first, third, and fifth transmembrane segments in the fourth domain (IVS1, IVS3, and IVS5) of Na_v1.8, respectively. A strong reticulum-like staining pattern consistent with the accumulation of protein in the ER was observed for the chimeric proteins including FLAG-TFR1(TM_{IVS1})-Myc and FLAG-TFR1(TM_{IVS3})-Myc (Fig. 1C). The expressed FLAG-TFR1(TM_{IVS3})-Myc was co-localized with the ER marker calnexin (Fig. 1E). In contrast, the chimeric protein FLAG-TFR1(TM_{IVS5})-Myc showed distinct surface expression (Fig. 1C). Consistent with the above observation, non-permeabilized immunostaining with Myc antibody showed that FLAG-TFR1-Myc and FLAG-TFR1(TM_{IVS5})-Myc exhibited prominent surface labeling in transfected COS-7 cells, whereas FLAG-TFR1(TM_{IVS1})-Myc and FLAG-TFR1(TM_{IVS3})-Myc displayed very faint surface labeling (Fig. 1C). The differences in surface labeling were not due to different levels of protein expression, because all constructs had a comparable expression level for permeabilized staining. The above morphological results were quantified by the ratio of the intensity from non-permeabilized (surface) to permeabilized (total) immunostaining. The statistical data revealed that the surface expression levels of FLAG-TFR1(TM_{IVS1})-Myc and FLAG-TFR1(TM_{IVS3})-Myc were significantly lower than that of FLAG-TFR1-Myc and FLAG-TFR1(TM_{IVS5})-Myc (Fig. 1D). Thus, the first and third transmembrane segments of the fourth domain display ER-localization activity. Then we detected ER-localization activity of the odd transmembrane segments in the left three domains of Na_v1.8 using the same strategy. The statistical results showed that the first and third transmembrane segments in the other three domains also largely restricted the surface expression of chimeric proteins (Fig. 1D). Our results suggest that the odd transmembrane segments of Na_v1.8 possess ER-localization activity.

We adopted the CD8 α system to detect ER-localization activity of the even transmembrane segments in Na_v1.8. To ensure availability of the CD8 α system, we created a chimeric protein Myc-CD8 α (TM_{AChR-S1}) in which the transmembrane segment of CD8 α was substituted by the first transmembrane segment of nicotinic acetylcholine receptors (AChR). An ER-retention/retrieval motif PLYFXXN conserved in the first transmembrane segment of nicotinic AChR restricts the surface expression of unassembled subunits (18). Consistent with their finding, we found that Myc-CD8 α (TM_{AChR-S1}) accumulated in the ER of transfected COS-7 cells and Myc-CD8 α (TM_{AChR-S1m}) with PLYFXXN mutated to alanines showed about a 10-fold increase in surface expression (Fig. 2B). Then we applied this system for detecting ER-localization

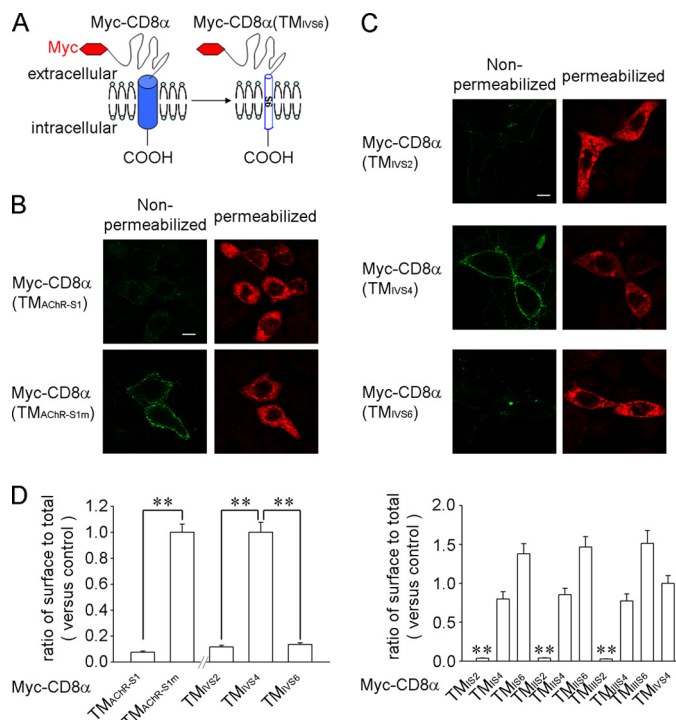


FIGURE 2. The even transmembrane segments of Na_v1.8 retain chimeric proteins in the ER. A, schematic diagrams showing the structure of CD8 α and CD8 α chimeric protein with the transmembrane segment substituted with the even transmembrane segment of Na_v1.8. B and C, the CD8 α screening system was verified and the effects of even transmembrane segments in the fourth domain of Na_v1.8 on the surface expression of chimeric proteins were analyzed. The plasmids expressing Myc-CD8 α (TM_{AChR-S1}) or Myc-CD8 α (TM_{AChR-S1m}) or Myc-CD8 α (TM_{IVS2}), Myc-CD8 α (TM_{IVS4}), or Myc-CD8 α (TM_{IVS6}) were transfected into COS-7 cells, respectively. The non-permeabilized (green) and permeabilized (red) immunofluorescence staining was carried out using mouse- and rabbit-derived antibodies against Myc, respectively. The images represent at least three independent experiments. Scale bar, 10 μ m. D, the statistical results (mean \pm S.E.) of surface (non-permeabilized) versus total (permeabilized) protein plotted as a percentage of control based on at least 45 cells in three experiments. **, $p < 0.01$ versus control cells or cells transfected with the plasmid of Myc-CD8 α (TM_{IVS4}).

activity of the second, fourth, and sixth transmembrane segments in the fourth domain (IVS2, IVS4, and IVS6) of Na_v1.8. Myc-CD8 α (TM_{IVS2}), Myc-CD8 α (TM_{IVS4}), and Myc-CD8 α (TM_{IVS6}) all showed a ER-localization pattern (Fig. 2C). However, the non-permeabilized immunostaining and the quantitative data showed that surface expression of Myc-CD8 α (TM_{IVS4}) was much stronger than Myc-CD8 α (TM_{IVS2}) and Myc-CD8 α (TM_{IVS6}) (Fig. 2, C and D), indicating that the second and sixth transmembrane segments in the fourth domain of Na_v1.8 exhibit much higher ER-localization activity than the fourth transmembrane segment. We further searched the remaining even transmembrane segments and found that only the second transmembrane segments in the left three domains greatly reduced the surface expression of chimeric protein (Fig. 2D). Thus, the even transmembrane segments of Na_v1.8 possess ER-localization activity.

Acidic Amino Acids in the Odd Transmembrane Segments Are Crucial for ER Localization—We performed alanine screening to map the amino acids responsible for ER localization in the odd transmembrane segments of Na_v1.8. The transmembrane segments were divided into three parts, which were mutated to alanines, respectively. As an example, we divided

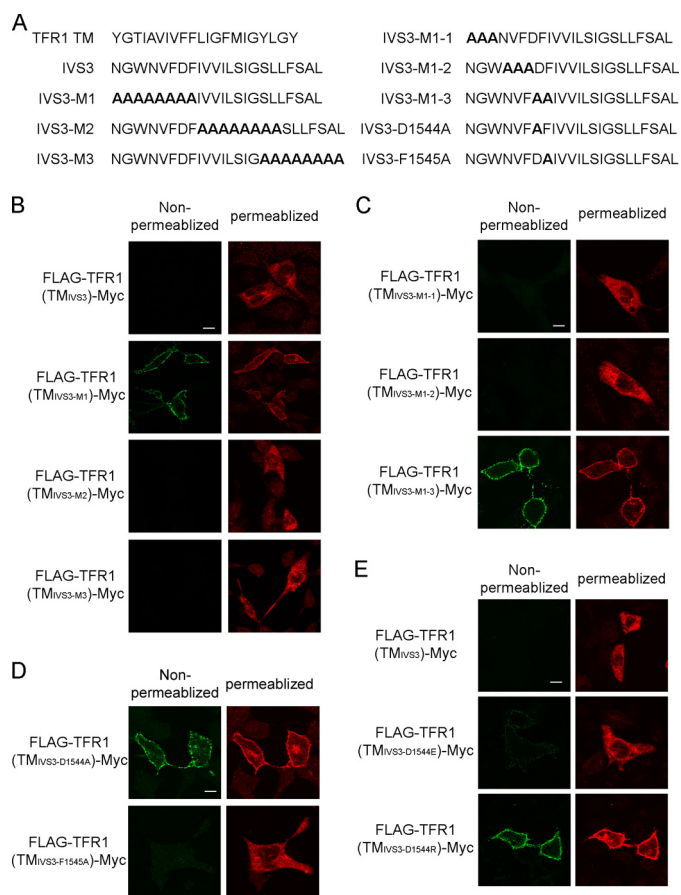


FIGURE 3. The acidic amino acid aspartate is critical for ER localization in the third transmembrane segment of the fourth domain. *A*, schematic representation of the amino acid sequences of TFR1 transmembrane segment, the third transmembrane segment in the fourth domain of Na_v1.8 and its mutants. *B–E*, alanine-scanning analysis was performed to determine the critical sequence for ER localization of the third transmembrane segment in the fourth domain. Plasmids expressing FLAG-TFR1(TM_{IVS3})-Myc or a series of mutants were transfected into COS-7 cells, respectively. Non-permeabilized (green) and permeabilized (red) immunofluorescence staining was carried out using mouse- and rabbit-derived antibodies against Myc, respectively. The representative images were chosen from at least three independent experiments. Scale bar, 10 μm.

the third transmembrane segment in the fourth domain into three parts (IVS3-M1, IVS3-M2, and IVS3-M3) and mutated each part to alanines in the chimeric protein. In COS-7 cells, the expressed FLAG-TFR1(TM_{IVS3-M2})-Myc and FLAG-TFR1(TM_{IVS3-M3})-Myc showed faint surface labeling (Fig. 3, *A* and *B*). In contrast, the expressed FLAG-TFR1(TM_{IVS3-M1})-Myc displayed marked surface labeling, indicating the potential ER-localization amino acids embedded in the first eight amino acids of the third transmembrane segment (Fig. 3, *A* and *B*). We further narrowed the location of the functional amino acids. FLAG-TFR1(TM_{IVS3-M1-3})-Myc showed strong surface labeling compared with FLAG-TFR1(TM_{IVS3-M1-1})-Myc and FLAG-TFR1(TM_{IVS3-M1-2})-Myc (Fig. 3, *A* and *C*), suggesting a potential role of aspartate (D) at 1544 and phenylalanine (F) at 1545 in ER localization. Finally, alanine substitution of the acidic amino acid aspartate in FLAG-TFR1(TM_{IVS3-D1544A})-Myc, other than the aromatic amino acid phenylalanine in FLAG-TFR1(TM_{IVS3-F1545A})-Myc, resulted in distinct surface labeling (Fig. 3, *A* and *D*). Charged amino acid residues in the

transmembrane segment have been reported to target membrane proteins for ER localization (17). However, ER-localization activity of the third transmembrane segment in the fourth domain disappeared when the acidic amino acid aspartate was mutated to the basic amino acid arginine but not the acidic amino acid glutamate (E) (Fig. 3*E*), suggesting the relative specificity of this acidic amino acid. Thus, the acidic amino acid aspartate is responsible for ER-localization activity of the third transmembrane segment.

By sequence alignment, we found that acidic amino acid aspartate or glutamate are conserved in the first and third transmembrane segments of the left three domains except the first one in the first domain (IS1) of Na_v1.8 (Fig. 4*A*). However, alanine substitution analysis showed that the single acidic amino acid was only responsible for ER localization in the third transmembrane segment of the third domain (IIIS3) and the first transmembrane segment of the fourth domain (IVS1) but not in other transmembrane segments (Fig. 4, *B* and *C*). Instead, motifs containing acidic amino acids were required for ER localization in those transmembrane segments, namely the DPFXE motif for the first transmembrane segment in the second domain (IIS1) and the NIXD motif for the third transmembrane segment in the second domain (IIS3). When these motifs were mutated to alanines, the chimeric proteins were expressed on the cell surface (Fig. 4*D*). These data strongly suggest that the acidic amino acids are critical for ER localization of odd transmembrane segments in Na_v1.8.

To analyze the influence of ER-localization amino acids in the transmembrane segments on the surface expression of full-length Na_v1.8, we performed alanine substitution for each ER-localization amino acid or motifs to get five mutants, including Na_v1.8^{IIIS3-D1223A}-GFP, Na_v1.8^{IVS1-D1480A}-GFP, Na_v1.8^{IVS3-D1544A}-GFP, Na_v1.8^{IIS1-D663A/P644A/E667A}-GFP, and Na_v1.8^{IIS3-N729A/I730A/D732A}-GFP. We expressed Na_v1.8-GFP or its mutants to HEK293 cells because of the higher transfection efficiency in this cell line than the COS-7 cell line. Two days after transfection, cell-surface biotinylation and immunoblotting showed that the mutated channels caused a 3–4-fold increase in surface expression than the wild-type Na_v1.8 (Fig. 5, *A–C*). Next we detected whether the acidic ER-localization amino acid has additive effects to the previously identified ⁴⁹⁵RRR⁴⁹⁷ signal (31). We expressed Na_v1.8-GFP or Na_v1.8^{R495A/R496A/R497A}-GFP or Na_v1.8^{R495A/R496A/R497A&IVS3-D1544A}-GFP in HEK293 cells and observed a higher surface expression of Na_v1.8^{R495A/R496A/R497A&IVS3-D1544A}-GFP than Na_v1.8^{R495A/R496A/R497A}-GFP (Fig. 5, *D* and *E*), suggesting that the acidic ER-localization amino acid and RRR signal might function in different stages of channel trafficking and by different mechanisms. Taken together, these data suggest that the acidic amino acids in transmembrane segments prevent surface expression of Na_v1.8.

Acidic Amino Acid for ER Localization in Transmembrane Segment Accelerates Protein Degradation—A quality control process called ERAD guarantees the clearance of misfolded or unassembled proteins with prolonged retention in the ER (23–26). We tested whether proteins containing acidic amino acids in transmembrane segments could be degraded through

Trafficking Regulation for Na_v1.8

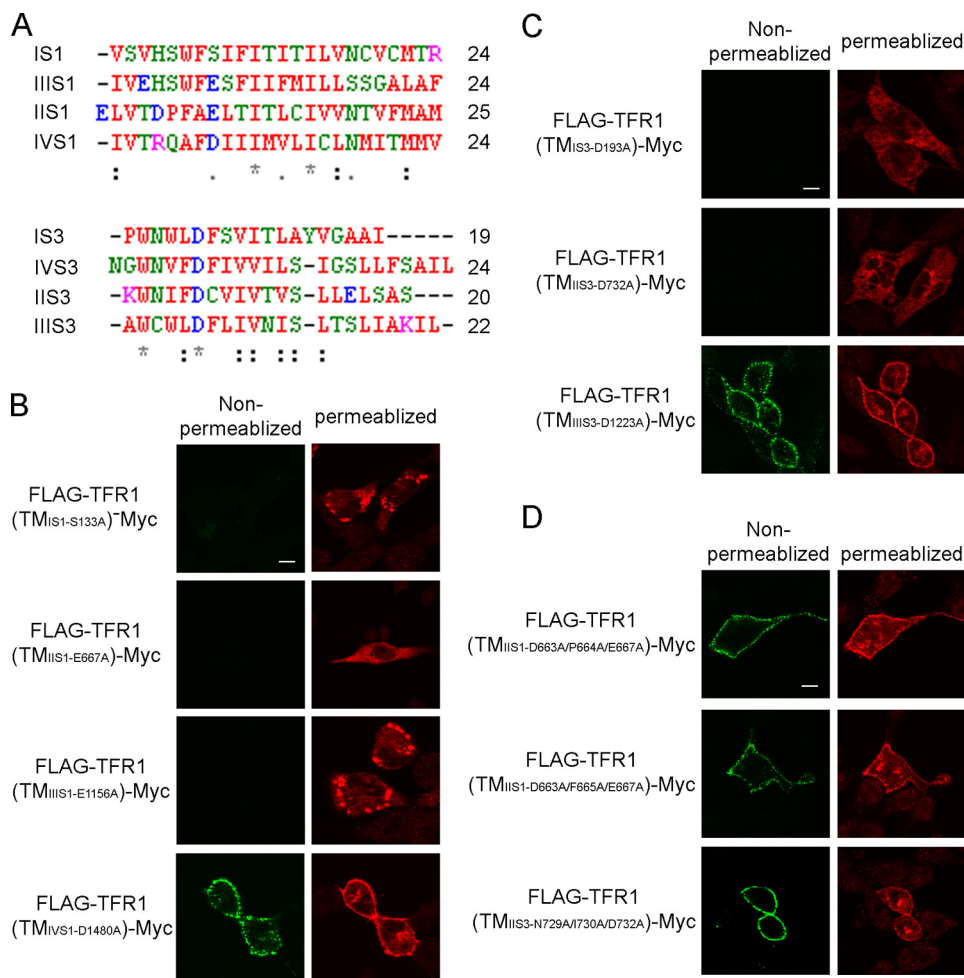


FIGURE 4. The acidic amino acid is also required for ER localization of other odd transmembrane segments. *A*, sequence alignment of the first and third transmembrane segments in each domain of Na_v1.8 shows that acidic amino acids (blue) are highly conserved. *B–D*, surface expression and subcellular localization of chimeric proteins with mutation of the acidic amino acid in the odd transmembrane segments analyzed. The plasmids expressing a series of TFR1 chimeric proteins with mutations of the acidic amino acids or acidic amino acid-containing motifs were transfected into COS-7 cells, respectively. Non-permeabilized (green) and permeabilized (red) immunofluorescence staining was performed using mouse- and rabbit-derived antibodies against Myc, respectively. The representative images are shown from at least three independent experiments. Scale bar, 10 μ m.

ERAD. We generated HEK293 cells stably expressing FLAG-TFR1(TM_{IVS3})-Myc or FLAG-TFR1(TM_{IVS3-D1544A})-Myc to avoid transient overexpression. The subcellular distribution of both chimeric proteins exhibited a similar pattern as that in transiently transfected COS-7 cells (data not shown). The degradation state was assayed by CHX chase in which cells were treated with CHX to stop protein synthesis, followed by immunoblotting to determine degradation rate. The protein level of FLAG-TFR1(TM_{IVS3})-Myc was decreased with a half-life of 1–2 h and nearly 90% of this chimeric protein was degraded at 12 h (Fig. 6A). However, FLAG-TFR1(TM_{IVS3-D1544A})-Myc remained stable even after a 12-h CHX treatment (Fig. 6A). Furthermore, full-length Na_v1.8 was also degraded rapidly in a comparable level with FLAG-TFR1(TM_{IVS3})-Myc, indicating the efficient elimination of this channel (Fig. 6B). In contrast, Na_v1.8_{IVS3-D1544A}-GFP displayed a much slower degradation speed (Fig. 6B). To detect the degradation state of endogenous Na_v1.8, we cultured DRG neurons from rat and analyzed the destiny of Na_v1.8. CHX chase assay showed that endogenous

Na_v1.8 was also degraded rapidly in DRG neurons but much slower than the expressed Na_v1.8-GFP in HEK293 cells (Fig. 6B), indicating an unknown mechanism to protect the channel from degradation. These results suggest that the acidic amino acid for ER localization in the transmembrane segment could increase protein degradation.

Ubiquitin-proteasome system is the key component in ERAD to degrade unwanted proteins (25, 38). We then focused on the role of the ubiquitin-proteasome system in degradation of FLAG-TFR1(TM_{IVS3})-Myc and full-length Na_v1.8. After a 6-h treatment with 10 μ M MG132, a proteasome inhibitor, the protein level of FLAG-TFR1(TM_{IVS3})-Myc and Na_v1.8-GFP stably expressed in HEK293 cells, and endogenous Na_v1.8 in DRG neurons were significantly elevated compared with the mutant form of FLAG-TFR1(TM_{IVS3-D1544A})-Myc at 6 h (Fig. 6C). MG132 treatment also increased the protein level of Na_v1.8_{IVS3-D1544A}-GFP with a less extent than that of Na_v1.8-GFP, suggesting the role of the acidic amino acid in promoting protein degradation and the existence of the remaining functional ER-localization motifs in Na_v1.8 (Fig. 6C). However, treatment with 100 μ M leupeptin, the inhibitor of lysosome, did not protect proteins from degradation (Fig. 6C). Correlatively, we found that the ubiquitination state of FLAG-TFR1(TM_{IVS3})-Myc and Na_v1.8-GFP in HEK293 cells was increased after MG132 treatment but not that of FLAG-TFR1(TM_{IVS3-D1544A})-Myc (Fig. 6D). The increase of the ubiquitination state in Na_v1.8_{IVS3-D1544A}-GFP after MG132 treatment was less than that in Na_v1.8-GFP (Fig. 6D). Therefore, these data indicate that proteins containing acidic amino acids in transmembrane segments are accelerated to degrade through ubiquitin-proteasome system.

Calnexin Is Involved in Degradation of Proteins Containing Acidic Amino Acids for ER Localization in Transmembrane Segments—Terminally misfolded and unassembled proteins were first recognized by ER chaperons such as calnexin/calreticulin, BiP, protein-disulfide isomerases or other factors, which are prerequisites for ERAD (23, 25). Because the acidic amino acids for ER localization are located in the transmembrane segments, we focused our attention in calnexin, which is a type I membrane protein. To establish whether calnexin is involved in quality control of proteins containing acidic amino

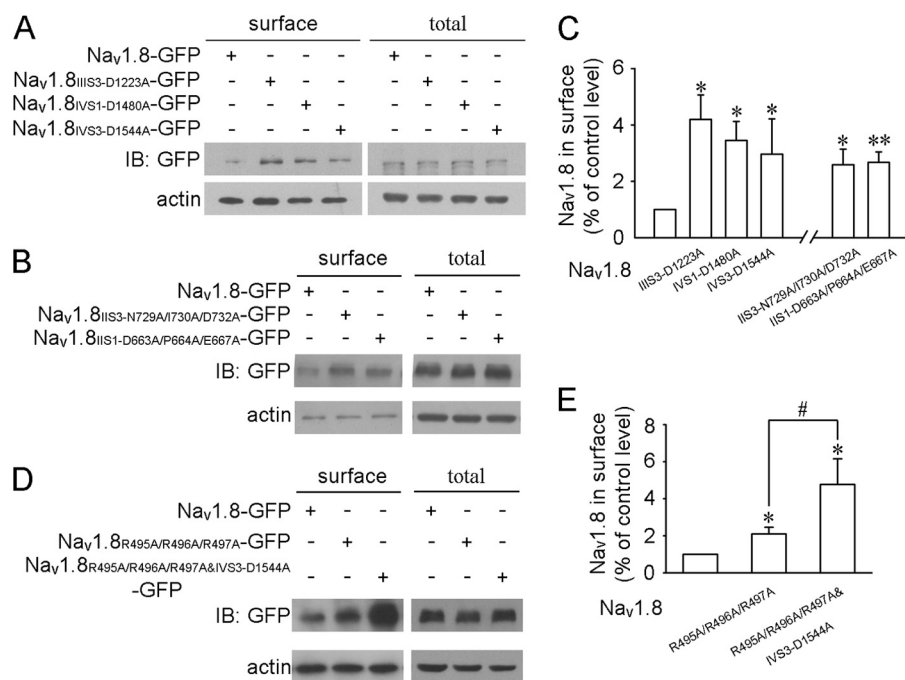


FIGURE 5. The acidic amino acids for ER localization in odd transmembrane segments reduce the surface expression of Na_v1.8. *A* and *B*, surface biotinylation analysis of Na_v1.8 and its mutants. The HEK293 cells were, respectively, transfected with plasmids expressing Na_v1.8-GFP or Na_v1.8 mutants substituting the identified ER-localization acidic amino acids with alanines, including Na_v1.8^{IIS3-N729A/I730A/D732A}-GFP, Na_v1.8^{IIS1-D663A/P664A/E667A}-GFP, Na_v1.8^{IIS3-D1223A}-GFP, Na_v1.8^{IVS1-D1480A}-GFP, and Na_v1.8^{IVS3-D1544A}-GFP, and subjected to cell surface biotinylation/immunoblotting (*IB*). Representative immunoblots are shown. Actin served as an internal control for protein loading. *C*, quantitative analysis of the above surface biotinylation data. The ratio (mean \pm S.E.) of immunoblot intensities of surface versus total proteins was calculated and data were plotted as a percentage of Na_v1.8-GFP ($n \geq 3$). *, $p < 0.05$; and **, $p < 0.01$ versus the cells transfected with Na_v1.8-GFP. *D* and *E*, the HEK293 cells were, respectively, transfected with plasmids expressing Na_v1.8-GFP or Na_v1.8^{R495A/R496A/R497A}-GFP or Na_v1.8^{R495A/R496A/R497A/IVS3-D1544A}-GFP and subjected to cell surface biotinylation/immunoblotting. Representative immunoblots are shown. Actin served as an internal control for protein loading. Quantitative analysis (mean \pm S.E.) was shown in *E* as described in *C*. *, $p < 0.05$ versus the cells transfected with Na_v1.8-GFP. #, $p < 0.05$ versus indicated.

acids for ER localization, we examined the interaction between calnexin and TFR1 chimeric proteins stably expressed in HEK293 cells. Using Myc antibody to immunoprecipitate TFR1 chimeric proteins, we found that binding of calnexin with FLAG-TFR1(TM_{IVS3})-Myc was much stronger than with its mutant form (Fig. 7A, left panel). To confirm this result, we performed the immunoprecipitation in reverse with antibody against calnexin and showed the same pattern (Fig. 7A, right panel). Moreover, to exclude the possibility that the weak interaction between calnexin and FLAG-TFR1(TM_{IVS3-D1544A})-Myc is due to their different subcellular localization, we artificially retained FLAG-TFR1(TM_{IVS3-D1544A})-Myc in the ER by adding an ER-retention/retrieval sequence MHRRRSR (39) to its N terminus (MHRRRSR-FLAG-TFR1(TM_{IVS3-D1544A})-Myc). The binding of calnexin with MHRRRSR-FLAG-TFR1(TM_{IVS3})-Myc was also much stronger than that with MHRRRSR-FLAG-TFR1(TM_{IVS3-D1544A})-Myc (Fig. 7B). Thus, calnexin recognizes the acidic amino acids for ER localization in the transmembrane segments.

We next detected whether the transmembrane segment of calnexin interacts with the third transmembrane segment in the fourth domain. The transmembrane segment of Myc-CD8 α was replaced by the same region of calnexin to get Myc-CD8 α (TM_{calnexin}) chimeric protein. In transiently expressed HEK293 cells, FLAG-TFR1(TM_{IVS3})-Myc interacted strongly

with Myc-CD8 α (TM_{calnexin}) but not with Myc-CD8 α , and FLAG-TFR1(TM_{IVS3-D1544A})-Myc exhibited a very weak binding with Myc-CD8 α (TM_{calnexin}) (Fig. 7C). To exclude the influence of different subcellular localization, the MHRRSR and KKTN motifs were added to the N terminus of the TFR1 chimeric proteins and the C terminus of CD8 α chimeric proteins to retain them in the ER, respectively (data not shown). We also found the strong interaction between MHRRSR-FLAG-TFR1(TM_{IVS3})-Myc and Myc-CD8 α (TM_{calnexin})-KKTN (Fig. 7D). Furthermore, we detected interaction of calnexin with full-length Na_v1.8 through its transmembrane segment in HEK293 cells (Fig. 7, E and F). Our data suggest that the transmembrane segment of calnexin interacts with the acidic amino acid-containing transmembrane segment of Na_v1.8.

To investigate the function of calnexin in the degradation of proteins containing acidic amino acids in the transmembrane segment, we overexpressed calnexin in HEK293 cells stably expressing FLAG-TFR1(TM_{IVS3})-Myc or Na_v1.8-GFP. We observed that the

steady-state levels of both proteins were decreased by calnexin overexpression but not calnexin(Δ C) (Fig. 7G), a mutant form of calnexin with deletion of the cytoplasmic tail, which was mislocated to the juxta-nuclear region instead of ER, whereas calnexin overexpression increased the expression level of FLAG-TFR1(TM_{IVS3-D1544A})-Myc (Fig. 7G). For the full-length channel, calnexin overexpression reduced the protein level of Na_v1.8^{IVS3-D1544A}-GFP but less than that of Na_v1.8-GFP (Fig. 7G). We next examined the expression levels of FLAG-TFR1(TM_{IVS3})-Myc, FLAG-TFR1(TM_{IVS3-D1544A})-Myc, and Na_v1.8-GFP under reduced calnexin levels by transfecting siRNA specific for human calnexin mRNA into the stably expressed HEK293 cells. Consistent with the above calnexin overexpression results, down-regulation of endogenous calnexin increased the protein level of FLAG-TFR1(TM_{IVS3})-Myc and Na_v1.8-GFP but decreased that of FLAG-TFR1(TM_{IVS3-D1544A})-Myc (Fig. 7H). Also, the increased level of Na_v1.8^{IVS3-D1544A}-GFP after down-regulating calnexin was less than that of Na_v1.8-GFP (Fig. 7H). The altered expression levels were rescued by the co-transfected calnexin mutant, which was resistant to siRNA, eliminating the off-target effect of calnexin siRNA (Fig. 7H). To further verify the conclusion, another strategy was performed. We generated two types of HEK293 cells stably expressing the shRNA construct designed to decrease endogenous calnexin (calnexin shRNA) or the shRNA

Trafficking Regulation for Na_v1.8

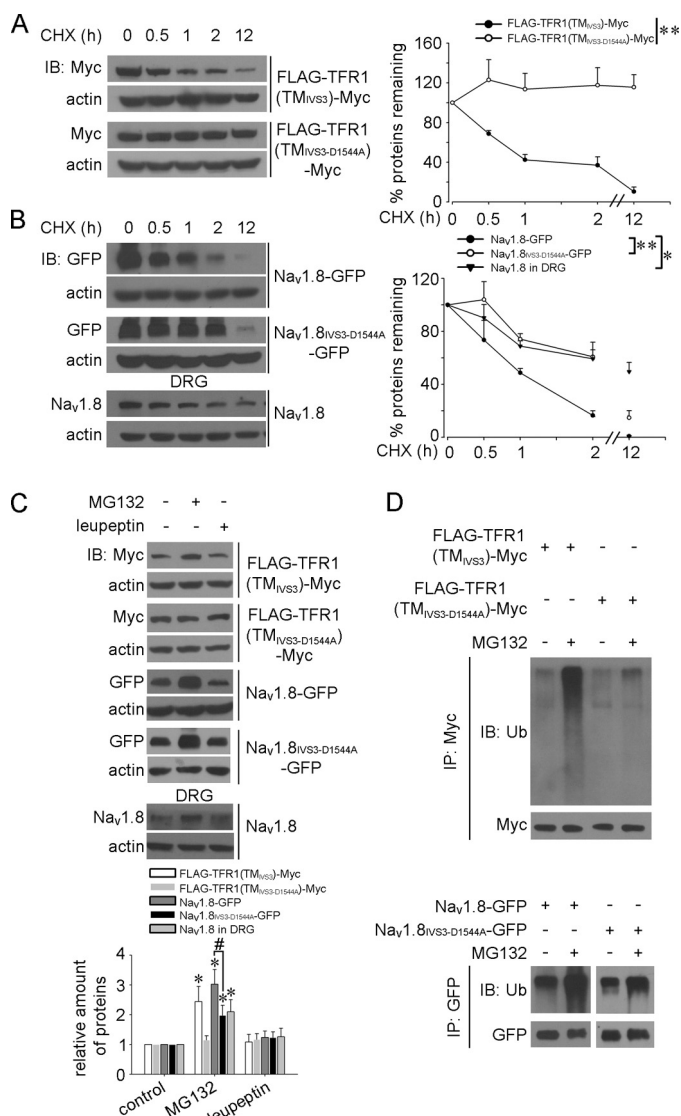


FIGURE 6. The acidic amino acids for ER localization in the transmembrane segments result in rapid degradation of proteins through ubiquitin-proteasome pathway. *A* and *B*, HEK293 cells or DRG cells were treated with 100 μ g/ml of CHX for the indicated time and subjected to immunoblotting. Representative immunoblots and quantitative analysis (mean \pm S.E.) are shown. Actin served as an internal control for protein loading. *, $p < 0.05$; **, $p < 0.01$, two-way analysis of variance. *C*, inhibition of proteasome but not lysosome pathway increases the protein level of expressed FLAG-TFR1(TM_{IVS3})-Myc and Nav1.8-GFP, and endogenous Nav1.8. The HEK293 cells stably expressing FLAG-TFR1(TM_{IVS3})-Myc or FLAG-TFR1(TM_{IVS3-D1544A})-Myc or Nav1.8-GFP or Nav1.8_{IVS3-D1544A}-GFP and DRG neurons were treated with 10 μ M MG132 or 100 μ M leupeptin for 6 h and subjected to immunoblotting. Representative immunoblots and quantitative analysis are shown. Actin served as an internal control for protein loading. Quantitative data (mean \pm S.E.) were plotted as a percentage of control. *, $p < 0.05$ versus the control cells ($n \geq 3$). #, $p < 0.05$ versus indicated. *D*, the ubiquitination state of expressed FLAG-TFR1(TM_{IVS3})-Myc and Nav1.8-GFP is increased after inhibition of ubiquitin-proteasome pathway. The HEK293 cells stably expressing FLAG-TFR1(TM_{IVS3})-Myc or FLAG-TFR1(TM_{IVS3-D1544A})-Myc or Nav1.8-GFP or Nav1.8_{IVS3-D1544A}-GFP were treated with 10 μ M MG132 for 6 h. Proteins were immunoprecipitated with Myc- or GFP-specific antibodies and then subjected to immunoblotting with antibodies against ubiquitin or Myc or GFP as indicated. Representative immunoblots are shown.

construct with the scrambled sequence (scramble shRNA). We found that the expression level of transiently expressed FLAG-TFR1(TM_{IVS3})-Myc and Nav1.8-GFP was elevated but the expressed FLAG-TFR1(TM_{IVS3-D1544A})-Myc was decreased in

HEK293 cells with reduced calnexin level (Fig. 7*I*). Although transiently expressed Nav1.8_{IVS3-D1544A}-GFP was elevated with down-regulated calnexin, the increased level was much less than Nav1.8-GFP (Fig. 7*I*). These data suggest that calnexin acts as a "pro-degradative" factor for FLAG-TFR1(TM_{IVS3})-Myc and Nav1.8 but as a protective factor for FLAG-TFR1(TM_{IVS3-D1544A})-Myc. Thus, calnexin promotes the degradation of proteins containing acidic amino acids for ER localization in transmembrane segments.

DISCUSSION

In this study, we have demonstrated that the transmembrane segments of Nav1.8 contribute to its ER localization and strictly control surface expression and the protein level of this channel. The acidic amino acids in the odd transmembrane segments are critical for ER localization and rapid degradation of Nav1.8. We have also presented strong evidence for interaction between the transmembrane segment of the ER chaperon calnexin and the odd transmembrane segments of Nav1.8. Overexpression or down-regulation of calnexin results in accelerated or decreased degradation speed of proteins containing acidic amino acids in odd transmembrane segments. These findings provide a novel mechanism for the quality control pathway of Nav1.8 and enlighten the trafficking process of proteins containing multiple transmembrane domains.

Nav1.8 Contains ER-localization Amino Acids in the Transmembrane Segments—Previous studies have reported that transmembrane segments contribute to ER localization of several membrane proteins. Transmembrane segments of the NMDA receptor (19), T cell antigen receptor α chains (15), AChR α subunit (18), a type III ER membrane protein Sec71p (40), and γ -secretase subunit PS enhancer 2 (41) contain important information for ER localization. Those findings demonstrate that the polar or even charged amino acids in the hydrophobic transmembrane segments are crucial for protein localization in ER. In our study, we identify a critical role of the acidic amino acids or motifs in ER localization in the odd transmembrane segments of Nav1.8, the same orientation as the type II membrane protein. However, the ER-localization signals in previous studies are mainly located in the transmembrane segments orientated as the type I membrane protein. Moreover, ER-localization activity of the third transmembrane segment disappeared when the acidic amino acid aspartate was mutated to the basic amino acid arginine. Thus, our data suggest a relative novelty and specificity of this acidic amino acid signal for ER localization.

In our previous work, we have found an RRR ER-retention/retrieval motif in the first intracellular loop of Nav1.8 (31). Now we also identify multiple acidic amino acids or acidic amino acid-containing motifs for ER localization in transmembrane segments of this channel. The phenomenon that multiple discrete ER-localization signals are present in one protein is not unprecedented. Two RXR ER-retention/retrieval signals in both the intracellular loop and C terminus of kainate receptor KA2 subunit have been found to regulate its surface expression (13, 42). Both the third transmembrane segment and C terminus of the NMDA NR1 subunit contain signals that localize the unassembled subunit in the ER (19, 43). The exact explanation

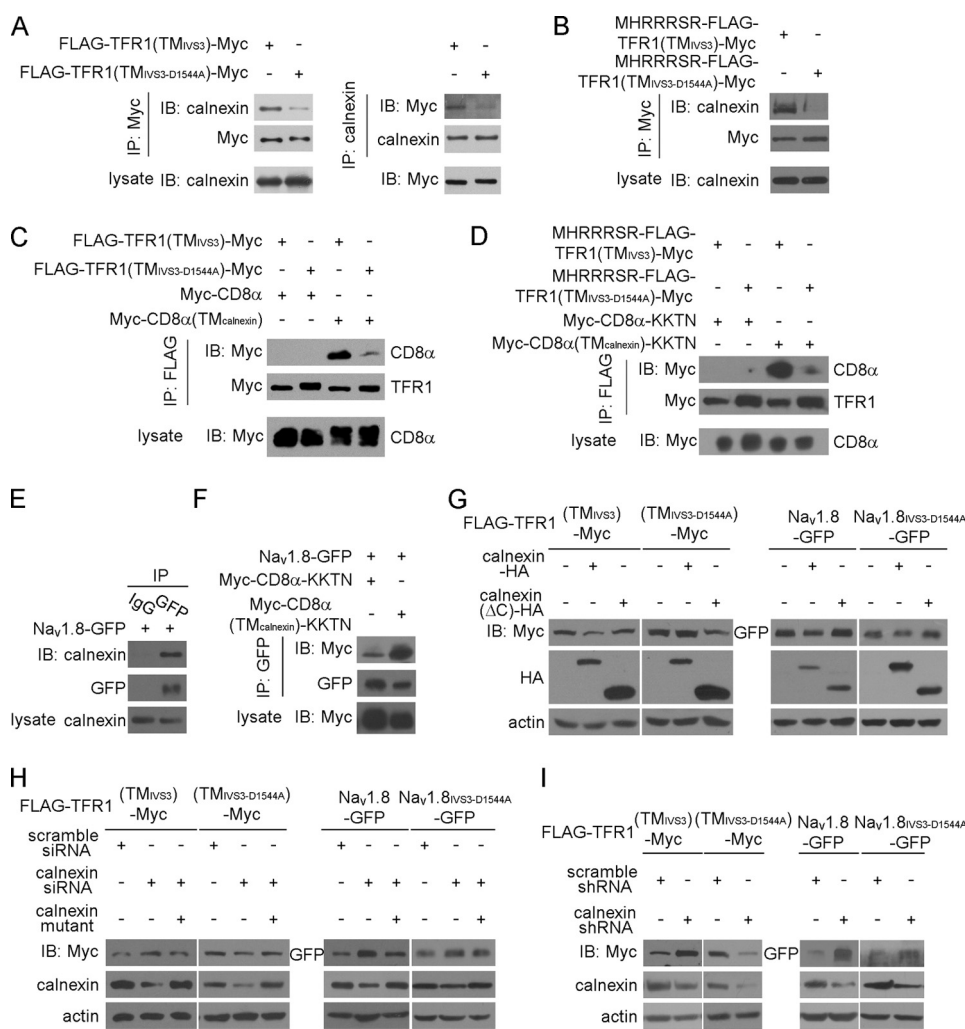


FIGURE 7. Calnexin mediates the degradation of proteins containing the acidic amino acid in the transmembrane segments. *A*, the expressed FLAG-TFR1(TM_{IVS3})-Myc interacts more strongly with calnexin than its mutant form FLAG-TFR1(TM_{IVS3-D1544A})-Myc. In HEK293 cells stably expressing FLAG-TFR1(TM_{IVS3})-Myc or FLAG-TFR1(TM_{IVS3-D1544A})-Myc, proteins were immunoprecipitated (IP) with Myc-specific antibody (*left panel*) or calnexin-specific antibody (*right panel*) and the cell lysates were subject to immunoblotting (IB) with antibodies against Myc or calnexin as indicated. Representative immunoblots are shown. *B*, in HEK293 cells transiently expressing MHRRRSR-FLAG-TFR1(TM_{IVS3})-Myc or MHRRRSR-FLAG-TFR1(TM_{IVS3-D1544A})-Myc, proteins were immunoprecipitated with Myc-specific antibody and the cell lysates were subject to immunoblotting with antibodies against Myc or calnexin. *C* and *D*, the transmembrane segment of calnexin interacts strongly with the third transmembrane segment in the fourth domain of Na_v1.8. The HEK293 cells transfected with various plasmids as indicated were subjected to co-immunoprecipitation assay. Proteins were immunoprecipitated with FLAG-specific antibody and the cell lysates were detected with antibody against Myc. *E*, Na_v1.8 interacts with calnexin. The HEK293 cells stably expressing Na_v1.8-GFP were immunoprecipitated with IgG or GFP-specific antibody and the cell lysates were analyzed with antibodies against GFP or calnexin as indicated. *F*, Na_v1.8 interacts with the isolated transmembrane segment of calnexin in the chimeric protein. The HEK293 cells stably expressing Na_v1.8-GFP were transfected with Myc-CD8α-KKTN or Myc-CD8α(TM_{calnexin})-KKTN plasmids, respectively. Proteins were immunoprecipitated with GFP-specific antibody and the cell lysates were probed with antibodies against GFP or Myc as indicated. *G*, overexpression of calnexin decreases the protein levels of FLAG-TFR1(TM_{IVS3})-Myc and Na_v1.8-GFP. The HEK293 cells stably expressing FLAG-TFR1(TM_{IVS3})-Myc or FLAG-TFR1(TM_{IVS3-D1544A})-Myc or Na_v1.8-GFP or Na_v1.8_{IVS3-D1544A}-GFP were transfected with the indicated plasmids. Immunoblotting analysis was performed with antibodies against Myc, GFP, HA, or actin as indicated. *H* and *I*, down-regulation of calnexin increases the protein level of FLAG-TFR1(TM_{IVS3})-Myc and Na_v1.8-GFP. The HEK293 cells stably expressing FLAG-TFR1(TM_{IVS3})-Myc or FLAG-TFR1(TM_{IVS3-D1544A})-Myc or Na_v1.8-GFP or Na_v1.8_{IVS3-D1544A}-GFP were transfected with the indicated siRNAs and mock vectors or vectors encoding the calnexin mutant in which two nucleotides were mutated to be resistant to calnexin siRNA (*H*). The HEK293 cells stably expressing calnexin shRNA or scramble shRNA were transfected with FLAG-TFR1(TM_{IVS3})-Myc or FLAG-TFR1(TM_{IVS3-D1544A})-Myc or Na_v1.8-GFP or Na_v1.8_{IVS3-D1544A}-GFP (*I*). The cell lysates were analyzed by immunoblotting with antibodies against Myc, GFP, calnexin, or actin as indicated.

transmembrane segment to the RRR signal in the intracellular loop on the surface expression of Na_v1.8 support this hypothesis. Each ER-localization signal could bind to a specific protein in the ER or Golgi, which may be regulated by various physiological stimulations and cause varying levels of channel trafficking from the ER. Another alternative explanation is that cells simply utilize redundant ER-localization signals to tightly control the surface expression of those critical receptors and ion channels.

Calnexin Recognizes the Transmembrane Segment Containing Acidic Amino Acid—The ER lectin chaperon calnexin has been implicated in monitoring and assisting the folding of glycoproteins, retaining misfolded or unassembled glycoproteins in the ER, and targeting persistently unfolded glycoproteins for ERAD (29, 44–45). The classical model proposes that calnexin can recognize the monoglucosylated structure (Glc₁Man₉GlcNAc₂ glycan form) of glycoproteins to facilitate protein folding and detect mannose-trimmed substrates (Man₈GlcNAc₂ glycan form) to promote protein degradation (29). Recently more and more data support the view that calnexin can also interact with folding glycoproteins through the polypeptide segments besides the glycan sites (35, 45, 46). In this study, we find that calnexin strongly interacts with chimeric proteins containing acidic amino acids in the transmembrane segment, and show that the isolated transmembrane segment of calnexin maintains this interaction. Importantly, the transmembrane segment of calnexin interacts with full-length Na_v1.8, suggesting that the binding transmembrane segments are exposed in the outer edge of this channel. This hypothesis is supported by the three-dimensional model of the voltage-gated sodium channel from single-particle image

analysis of the cryoelectron microscope. In the model, the first, second, and third transmembrane segments in each domain form the outer edge of the channel, and the fourth transmembrane segment is located in the center (47–48). Thus, our

analysis of the cryoelectron microscope. In the model, the first, second, and third transmembrane segments in each domain form the outer edge of the channel, and the fourth transmembrane segment is located in the center (47–48). Thus, our

Trafficking Regulation for Na_v1.8

results provide the first direct evidence that the transmembrane segment of calnexin mediates the binding to its substrate.

Our data from “gain of function” and “loss of function” experiments reveal that calnexin enhances the degradation of FLAG-TFR1(TM_{IVS3})-Myc, whereas the mutant form FLAG-TFR1(TM_{IVS3-D1544A})-Myc is stabilized by calnexin. It is very interesting that calnexin plays opposite roles in two proteins with only one amino acid difference. The similar phenomenon has been observed when examining the impact of calnexin on the cystic fibrosis transmembrane conductance regulator (CFTR) and its ΔF508 variant (the most frequent mutation found in the patient with the genetic disease cystic fibrosis). Both wild-type and ΔF508 CFTR interact with calnexin. However, overexpression of calnexin has no effect on wild-type CFTR, but increases the degradation of ΔF508 CFTR (49). These data suggest that calnexin can discriminate the structural feature among different proteins.

Implications of Channel ER Localization—ER quality control machinery ensures that only properly folded proteins transport along the secretory pathway and inefficiently folded or misfolded proteins are finally degraded by ERAD pathway. A number of disease-related mutations often result in the production of structurally misfolded mutants that are rapidly degraded by ERAD (35, 50, 51). Interestingly, even wild-type proteins undergo inefficient folding, including CFTR (52), Shaker-type potassium channels (53), and epithelial sodium channels (54). In this study, we identify Na_v1.8 as another target of ERAD. One common explanation is that overvigilant ER quality control is employed to strictly control protein expression on the cell surface. Our data support another possibility that expression of Na_v1.8 can be regulated by other unknown proteins to escape the ER quality control process. In supporting this point, the degradation speed of endogenous Na_v1.8 in DRG neurons is slower than that in transfected HEK293 cells, suggesting that some neuron-specific proteins may be involved in protecting Na_v1.8 from rapid degradation. Identification of those proteins could help us to understand mechanisms of Na_v1.8 trafficking regulation in physiological conditions.

So far, an increasing number of voltage-gated sodium channel mutations (channelopathies) have been verified to be associated with many inherited disorders such as epilepsy and heart arrhythmias (55). Surprisingly many disease-related mutations are located within or very close to the transmembrane segments of sodium channels (56). The transmembrane segments are highly conserved among voltage-gated sodium channel subtypes, including acidic amino acids or the acidic amino acid-containing motifs identified in our experiments. If any mutations are related to the acidic amino acid, the trafficking and degradation state of the channel mutant may be changed. One such example comes from research on GABA_A receptor α1 subunit with a non-conservative missense mutation A322D in the third transmembrane segment, leading to autosomal dominant juvenile myoclonic epilepsy. The A322D mutant resides in the ER and undergoes ERAD through the ubiquitin-proteasome system, resulting in reduced total and surface expression (57). Thus, our findings could shed light on understanding the mechanism relating sodium channel mutations in transmembrane segments to disease phenotype.

Acknowledgments—We appreciate Dr. Xu Zhang for critical comments on the experiments and manuscript. We also thank Dr. Xiang-Jun Tong for providing the original plasmid of TFR1 and Ying-Liang Wei and Jiao Li for help in some experiments.

REFERENCES

1. Goldin, A. L. (2001) *Annu. Rev. Physiol.* **63**, 871–894
2. Wood, J. N., Boorman, J. P., Okuse, K., and Baker, M. D. (2004) *J. Neurobiol.* **61**, 55–71
3. Ogata, N., and Ohishi, Y. (2002) *Jpn. J. Pharmacol.* **88**, 365–377
4. Goldin, A. L., Barchi, R. L., Caldwell, J. H., Hofmann, F., Howe, J. R., Hunter, J. C., Kallen, R. G., Mandel, G., Meisler, M. H., Netter, Y. B., Noda, M., Tamkun, M. M., Waxman, S. G., Wood, J. N., and Catterall, W. A. (2000) *Neuron* **28**, 365–368
5. Djouhri, L., Fang, X., Okuse, K., Wood, J. N., Berry, C. M., and Lawson, S. N. (2003) *J. Physiol.* **550**, 739–752
6. Gold, M. S., Weinreich, D., Kim, C. S., Wang, R., Treanor, J., Porreca, F., and Lai, J. (2003) *J. Neurosci.* **23**, 158–166
7. Khasar, S. G., Gold, M. S., and Levine, J. D. (1998) *Neurosci. Lett.* **256**, 17–20
8. Akopian, A. N., Souslova, V., England, S., Okuse, K., Ogata, N., Ure, J., Smith, A., Kerr, B. J., McMahon, S. B., Boyce, S., Hill, R., Stanfa, L. C., Dickenson, A. H., and Wood, J. N. (1999) *Nat. Neurosci.* **2**, 541–548
9. Lai, J., Gold, M. S., Kim, C. S., Bian, D., Ossipov, M. H., Hunter, J. C., and Porreca, F. (2002) *Pain* **95**, 143–152
10. Zerangue, N., Schwappach, B., Jan, Y. N., and Jan, L. Y. (1999) *Neuron* **22**, 537–548
11. Margeta-Mitrovic, M., Jan, Y. N., and Jan, L. Y. (2000) *Neuron* **27**, 97–106
12. Bichet, D., Cornet, V., Geib, S., Carlier, E., Volsen, S., Hoshi, T., Mori, Y., and De Waard, M. (2000) *Neuron* **25**, 177–190
13. Nasu-Nishimura, Y., Hurtado, D., Braud, S., Tang, T. T., Isaac, J. T., and Roche, K. W. (2006) *J. Neurosci.* **26**, 7014–7021
14. Nilsson, T., Jackson, M., and Peterson, P. A. (1989) *Cell* **58**, 707–718
15. Bonifacino, J. S., Cosson, P., and Klausner, R. D. (1990) *Cell* **63**, 503–513
16. Bonifacino, J. S., Suzuki, C. K., and Klausner, R. D. (1990) *Science* **247**, 79–82
17. Bonifacino, J. S., Cosson, P., Shah, N., and Klausner, R. D. (1991) *EMBO J.* **10**, 2783–2793
18. Wang, J. M., Zhang, L., Yao, Y., Viroonchatapan, N., Rothe, E., and Wang, Z. Z. (2002) *Nat. Neurosci.* **5**, 963–970
19. Horak, M., Chang, K., and Wenthold, R. J. (2008) *J. Neurosci.* **28**, 3500–3509
20. Stevens, T. L., Blum, J. H., Foy, S. P., Matsuuchi, L., and DeFranco, A. L. (1994) *J. Immunol.* **152**, 4397–4406
21. Qiu, S., Zhang, X. M., Cao, J. Y., Yang, W., Yan, Y. G., Shan, L., Zheng, J., and Luo, J. H. (2009) *J. Biol. Chem.* **284**, 20285–20298
22. Vacher, H., Mohapatra, D. P., Misonou, H., and Trimmer, J. S. (2007) *FASEB J.* **21**, 906–914
23. Meusser, B., Hirsch, C., Jarosch, E., and Sommer, T. (2005) *Nat. Cell Biol.* **7**, 766–772
24. Sayeed, A., and Ng, D. T. (2005) *Crit. Rev. Biochem. Mol. Biol.* **40**, 75–91
25. Raasi, S., and Wolf, D. H. (2007) *Semin. Cell Dev. Biol.* **18**, 780–791
26. Vembar, S. S., and Brodsky, J. L. (2008) *Nat. Rev. Mol. Cell Biol.* **9**, 944–957
27. Hammond, C., Braakman, I., and Helenius, A. (1994) *Proc. Natl. Acad. Sci. U.S.A.* **91**, 913–917
28. Ware, F. E., Vassilakos, A., Peterson, P. A., Jackson, M. R., Lehrman, M. A., and Williams, D. B. (1995) *J. Biol. Chem.* **270**, 4697–4704
29. Ellgaard, L., Molinari, M., and Helenius, A. (1999) *Science* **286**, 1882–1888
30. Renganathan, M., Cummins, T. R., and Waxman, S. G. (2001) *J. Neurophysiol.* **86**, 629–640
31. Zhang, Z. N., Li, Q., Liu, C., Wang, H. B., Wang, Q., and Bao, L. (2008) *J. Cell Sci.* **121**, 3243–3252
32. Novakovic, S. D., Tzoumaka, E., McGivern, J. G., Haraguchi, M., Sangameswaran, L., Gogas, K. R., Eglén, R. M., and Hunter, J. C. (1998) *J. Neurosci.* **18**, 2174–2187

33. Okuse, K., Malik-Hall, M., Baker, M. D., Poon, W. Y., Kong, H., Chao, M. V., and Wood, J. N. (2002) *Nature* **417**, 653–656
34. Collawn, J. F., Stangel, M., Kuhn, L. A., Esekogwu, V., Jing, S. Q., Trowbridge, I. S., and Tainer, J. A. (1990) *Cell* **63**, 1061–1072
35. Swanton, E., High, S., and Woodman, P. (2003) *EMBO J.* **22**, 2948–2958
36. Bao, L., Jin, S. X., Zhang, C., Wang, L. H., Xu, Z. Z., Zhang, F. X., Wang, L. C., Ning, F. S., Cai, H. J., Guan, J. S., Xiao, H. S., Xu, Z. Q., He, C., Hökfelt, T., Zhou, Z., and Zhang, X. (2003) *Neuron* **37**, 121–133
37. Tang, B. L., Low, S. H., and Hong, W. (1997) *Eur. J. Cell Biol.* **73**, 98–104
38. Römisch, K. (2005) *Annu. Rev. Cell Dev. Biol.* **21**, 435–456
39. Schutze, M. P., Peterson, P. A., and Jackson, M. R. (1994) *EMBO J.* **13**, 1696–1705
40. Sato, K., Sato, M., and Nakano, A. (2003) *Mol. Biol. Cell* **14**, 3605–3616
41. Kaether, C., Scheuermann, J., Fassler, M., Zilow, S., Shirotani, K., Valkova, C., Novak, B., Kacmar, S., Steiner, H., and Haass, C. (2007) *EMBO Rep.* **8**, 743–748
42. Ren, Z., Riley, N. J., Garcia, E. P., Sanders, J. M., Swanson, G. T., and Marshall, J. (2003) *J. Neurosci.* **23**, 6608–6616
43. Scott, D. B., Blanpied, T. A., Swanson, G. T., Zhang, C., and Ehlers, M. D. (2001) *J. Neurosci.* **21**, 3063–3072
44. Ellgaard, L., and Helenius, A. (2003) *Nat. Rev. Mol. Cell Biol.* **4**, 181–191
45. Williams, D. B. (2006) *J. Cell Sci.* **119**, 615–623
46. Ihara, Y., Cohen-Doyle, M. F., Saito, Y., and Williams, D. B. (1999) *Mol. Cell* **4**, 331–341
47. Cusdin, F. S., Clare, J. J., and Jackson, A. P. (2008) *Traffic* **9**, 17–26
48. Sato, C., Ueno, Y., Asai, K., Takahashi, K., Sato, M., Engel, A., and Fujiyoshi, Y. (2001) *Nature* **409**, 1047–1051
49. Farinha, C. M., and Amaral, M. D. (2005) *Mol. Cell. Biol.* **25**, 5242–5252
50. Hong, Z., Jin, H., Tzfira, T., and Li, J. (2008) *Plant Cell* **20**, 3418–3429
51. Kopito, R. R. (1999) *Physiol. Rev.* **79**, S167–173
52. Ward, C. L., Omura, S., and Kopito, R. R. (1995) *Cell* **83**, 121–127
53. Liu, T. I., Lebaric, Z. N., Rosenthal, J. J., and Gilly, W. F. (2001) *J. Neurophysiol.* **85**, 61–71
54. Weisz, O. A., Wang, J. M., Edinger, R. S., and Johnson, J. P. (2000) *J. Biol. Chem.* **275**, 39886–39893
55. George, A. L., Jr. (2005) *J. Clin. Invest.* **115**, 1990–1999
56. Meisler, M. H., and Kearney, J. A. (2005) *J. Clin. Invest.* **115**, 2010–2017
57. Gallagher, M. J., Ding, L., Maheshwari, A., and Macdonald, R. L. (2007) *Proc. Natl. Acad. Sci. U.S.A.* **104**, 12999–13004